



HAL
open science

On the Use of Fluxgate 3-Axis Magnetometers in Archaeology: Application with a Multi-sensor Device on the Site of Qasr ‘Allam in the Western Desert of Egypt

Bruno Gavazzi, Rozan Alkhatib-Alkontar, Marc Munschy, Frédéric Colin,
Catherine Duvette

► To cite this version:

Bruno Gavazzi, Rozan Alkhatib-Alkontar, Marc Munschy, Frédéric Colin, Catherine Duvette. On the Use of Fluxgate 3-Axis Magnetometers in Archaeology: Application with a Multi-sensor Device on the Site of Qasr ‘Allam in the Western Desert of Egypt. *Archaeological Prospection*, 2017, 24 (1), pp.59 - 73. 10.1002/arp.1553 . hal-01624846

HAL Id: hal-01624846

<https://hal.science/hal-01624846>

Submitted on 1 Feb 2021

HAL is a multi-disciplinary open access archive for the deposit and dissemination of scientific research documents, whether they are published or not. The documents may come from teaching and research institutions in France or abroad, or from public or private research centers.

L'archive ouverte pluridisciplinaire **HAL**, est destinée au dépôt et à la diffusion de documents scientifiques de niveau recherche, publiés ou non, émanant des établissements d'enseignement et de recherche français ou étrangers, des laboratoires publics ou privés.

**On the use of fluxgate 3-axis magnetometers in
archaeology: application with a multi-sensor device on the
site of Qasr 'Allam in the Western Desert of Egypt.**

Journal:	<i>Archaeological Propection</i>
Manuscript ID	ARP-16-0005.R1
Wiley - Manuscript type:	Research Article
Date Submitted by the Author:	n/a
Complete List of Authors:	Gavazzi, Bruno; Université de Strasbourg, Institut de Physique du Globe de Strasbourg; Université de Strasbourg, Archéologie et histoire ancienne : Méditerranée – Europe Alkhatib-Alkontar, Rozan; Université de Strasbourg, Institut de Physique du Globe de Strasbourg Munsch, Marc; Université de Strasbourg, Institut de Physique du Globe de Strasbourg Colin, Frédéric; Université de Strasbourg, Archéologie et histoire ancienne : Méditerranée – Europe; Institut Français d'Archéologie Orientale Duvette, Catherine; Université de Strasbourg, Archéologie et histoire ancienne : Méditerranée – Europe
Keywords:	Multi-sensors, Magnetic compensation, Magnetometry, 3-axis fluxgate magnetometers, Potential field transformations, Vertical vector fluxgate

1
2
3
4
5
6
7
8
9
10
11
12
13
14
15
16
17
18
19
20
21
22
23
24
25
26
27
28
29
30
31
32
33
34
35
36
37
38
39
40
41
42
43
44
45
46
47
48
49
50
51
52
53
54
55
56
57
58
59
60

1 **On the use of fluxgate 3-axis magnetometers in archaeology: application with a**
2 **multi-sensor device on the site of Qasr 'Allam in the Western Desert of Egypt.**

3 Bruno Gavazzi (corresponding author)^{a, b} (bgavazzi@unistra.fr ; Phone +33368850473 ;
4 mobile +33607639713), Rozan Alkhatib-Alkontar^a, Marc Munsch^a, Frédéric Colin^{b, c},
5 Catherine Duvette^b

6 ^aUMR 7516, Institut de Physique du Globe de Strasbourg (IPGS), École et Observatoire
7 des Sciences de la Terre (EOST), University of Strasbourg, Bâtiment Blessig, 1 rue
8 Blessig, F-67084 Strasbourg cedex, France.

9 ^bUMR 7044, Archéologie et histoire ancienne : Méditerranée – Europe (Archimède),
10 Maison Interuniversitaire des Sciences de l'Homme – Alsace (MISHA), University of
11 Strasbourg, 5 allée du Général Rouvillois, F-67083 Strasbourg cedex, France.

12 ^cInstitut Français d'Archéologie Orientale (IFAO), 37 rue al-Cheikh Ali Youssef, B.P.
13 11562 Qasr al-Aïny 11441 Cairo, Egypt.

14 **Running head:** Fluxgate 3-axis magnetometers in archaeology: a multi-sensor device

15 **Sponsor:** The study was sponsored by the Initiatives d'Excellence (IdEx, Programme
16 Investissements d'Avenir) of the University of Strasbourg.

17 **Abstract**

18 Fluxgate 3-axis magnetometers are seldom used on archaeological sites due to their lack
19 of precision. Nonetheless, they offer light weight, low power consumption and the
20 ability of compensation of the magnetization of the prospecting device. This study
21 proposes to use calibration and compensation processes developed for space research
22 and aerial measurement to build a multi-sensors and georeferenced device to assess
23 deep and shallow objects for large scale archaeological investigations in Qasr 'Allam, in
24 a context of heavy sedimentary coverage and uneven surface. The use of the device on
25 the site in combination with potential field transformations of the signal such as the
26 double reduction to the pole and the vertical derivative reveal a vast irrigation system as
27 well as a large cultic facility. A comparison with gradiometric measurements shows a
28 resolution at least as good for shallow sources. The precise positioning allows to
29 perform targeted excavations which validate the geophysical interpretations and offer
30 new archaeological information. These discoveries give enough proof to the local
31 authorities to clearly delimit the area to be protected from the threatening progression of
32 agricultural fields.

33 **Keywords:** Magnetometry, 3-axis fluxgate magnetometers, Multi-sensors, Magnetic
34 compensation, Potential field transformations, Vertical vector fluxgate.

1
2
3
4
5
6
7
8
9
10
11
12
13
14
15
16
17
18
19
20
21
22
23
24
25
26
27
28
29
30
31
32
33
34
35
36
37
38
39
40
41
42
43
44
45
46
47
48
49

Introduction

Situated in the Western Desert of Egypt, the oasis of Bahariya (Figure 1) is inhabited since Prehistory (Svoboda, 2006; 2013). The main phases of the ancient Egyptian civilization can be observed in the area. However, they are not as well documented as in the Nile valley because only a few scholars have studied the Bahariya region. This is mainly due to access difficulties until construction of road infrastructure in the mid-20th century. The growing number of investigations took place since the end of the nineties. They revealed the archaeological potential of the area for illustration of a locally badly known period, ranging from the Third Intermediate Period to the Roman times, (i.e. from the 9th century B.C. to the 3rd century A.D. (Colin, 2013a, pp. 151–152)). This paper focuses on the site of Qasr ‘Allam (Figure 1), which integrity is threatened by heavy sedimentary processes and the rapid site destruction by recent increases in agricultural development. Geophysics is used to locate and study the archaeological remains of a historically significant dwelling.

The site of Qasr ‘Allam

Before any archaeological study, the site of Qasr ‘Allam was known mostly as a rectangular structure emerging from the sand which was interpreted by the inhabitant as an Arabic fort (Colin and Labrique, 2003, pp. 169–170). More than ten years of excavation then revealed facilities buried within sand and mud to be composed of mudbrick buildings of different natures, such as housings, storerooms and workshops (Figure 2, A-B-C). These structures were interpreted as part of a wide religious estate, the “Domain of Amun” according to stamped potteries found in the domestic dump sites of the dwellings. Two periods of occupation can be identified from 9th to 7th centuries B.C. (Colin, 2011, pp. 57–68). A complex network of fossilized irrigation structures can be identified through the traces of wells as well as open and underground channels surrounding the dwelling. In nowadays arid landscape most of these structures are partially or totally covered with sand. Often, only the materials excavated during construction and maintenance are visible on the surface (Figure 2, A-D-E-F).

These discoveries might indicate that the site could be a well preserved example of a complete cultic facility with three main components: a cultic core, associated domestic

1
2
3
4 66 buildings and its surrounding agricultural domain, of which most parts are still buried
5
6 67 within the ground. The structural organization of the excavated buildings suggests
7
8 68 indeed that they were only an annex in the periphery of a much larger and central
9
10 69 religious facility (Colin, 2011, pp. 65–66; Colin and Duvette, 2012, pp. 161–162).
11
12 70 According to this hypothesis, the direction of the access ramp of a cellular foundation
13
14 71 platform (Figure 2, A-B), whose typology is well known in the Nile valley (Spencer,
15
16 72 1979a, pp. 116–118; Spencer, 1979b; Traunecker, 1987; Leclère, 2008, pp. 630–636;
17
18 73 Malecka-Drozdz, 2014), would indicate that the presumed core is located westwards,
19
20 74 where lies a sand dune a few metres thick and where no archaeological traces are visible
21
22 75 on the surface.

23
24 76 However, this hypothesis suffers from two uncertainties: 1- the lack of traces on the
25
26 77 surface of the complex core; 2- the lack of information on the spatial and chronological
27
28 78 links between the buildings and the irrigation system.

29
30 79 Answers to these problems could be gained from a geophysical imaging of the sub-
31
32 80 surface. The surveying strategy should then take into account strong constraints: the
33
34 81 area is highly threatened from the west by the agricultural development, increasing
35
36 82 every year. Therewith, the whole dune shows an uneven topography scattered with dried
37
38 83 halfa grass and bushes reaching a height up to 0.8 m. Thus, the prospection of the area
39
40 84 must be fast and adapted to the roughness of the terrain.

41 42 85 **Choice of the geophysical method**

43
44 86 In such a context, the most appropriate solution would appear to be the magnetic
45
46 87 methods. Geomagnetism is a popular and effective method for archaeological purposes
47
48 88 (Linford, 2006; Gaffney, 2008). The main advantages are: -1- the anthropic traces show
49
50 89 usually a strong contrast of magnetization with their surroundings; -2- the rapidity of
51
52 90 measurement and light weight of the sensors to allow mapping of large surfaces with a
53
54 91 high density of data. In addition, a first prospection using vector gradiometer (Geoscan
55
56 92 FM256) was conducted between the sand dune and the platform in 2006 and 2010 by
57
58 93 Tomasz Herbich (Herbich, 2011). It revealed irrigation structures as well as walls and
59
60 94 foundation trenches (Colin, 2006; Colin, 2010; Herbich, 2011), thus giving evidence of
95
96 95 a contrast of magnetization strong enough to identify the archaeological remains.
97
98 96 However, the study of Herbich (2011) also revealed some limitations over the sand
99
100 97 dune: the topography and vegetation make the implementation of a grid and the

1
2
3
4 98 measurements less than 0.8 m above the ground highly difficult without an intense
5
6 99 preparation of the field. Moreover, one of the properties of the vertical gradient is to
7
8 100 enhance short wavelength and to smooth out large wavelength variations of the
9
10 101 magnetic field. This makes gradiometers extremely sensitive to shallow objects but of
11
12 102 limited capability to identify deeper sources or lower magnetic contrasts as it is the case
13
14 103 for Qasr ‘Allam (Blakely, 1995, pp. 324–326; Fagaly, 2001, pp. 327–328). This paper
15
16 104 proposes to overcome these limitations by adapting the measurement of the total
17
18 105 magnetic field with 3-axis vector fluxgate magnetometers, usually used in space
19
20 106 research or mining exploration (Nabighian *et al.*, 2005), and more recently for the
21
22 107 detection of unexploded ordnances (Munsch *et al.*, 2007), to archaeological surveys.

108 **Method**

109 *Device*

110 The core of the developed method lies in the measurement of the intensity of the
111 magnetic field with fluxgate magnetometers. Such magnetometers (Figure 3, A) have
112 the advantage of being light (80 g) and consuming low energy (< 1 W). Their three
113 orthogonal sensors allow the measurement of the three components of the magnetic
114 field at rate up to more than 1000 Hz (Primdahl, 1979), from which the total field can
115 easily be calculated. The device developed for this study (Figure 3, C) is built around an
116 in-house developed electronics (Figure 3, B). It powers the rest of the instrument,
117 digitizes and stores the data of 1 to 8 magnetometers as well as 1 to 2 global navigation
118 satellite system (GNSS) antennas. The electronics is mounted on a backpack and 4
119 magnetometers are placed 0.5 m apart from each other in front of the operator, one
120 metre above the ground. A GNSS antenna is placed at the top of the backpack for the
121 navigation. Both navigation and magnetic data are displayed in real time through a head
122 mounted display (HMD). The device weighs less than 15 kg and can be operated by a
123 single person who follows parallel survey lines set every 2 m and displayed in the
124 HMD. Thus, georeferenced magnetic profiles are acquired every 0.5 m centred on each
125 survey line without any preparation on the field. In Qasr ‘Allam, 5000 m² to 12000 m²
126 of magnetic data were acquired per hour of measurement.

127 *Calibration and compensation*

1
2
3
4 128 The major disadvantage of the fluxgate magnetometers is of being relative devices.
5
6 129 This means that the instrument requires a precise calibration before each session of
7
8 130 measurements to correct errors of sensitivity, offset and angle. This problem is well
9
10 131 known and various techniques of calibration have been developed. In this study the
11
12 132 calibration is done using a process developed initially for space research (Olsen *et al.*,
13
14 133 2003). It consists in the rotation of the magnetometers (or the whole device) in all
15
16 134 direction around a fixed point where the magnetic field can be considered steady. The
17
18 135 registered variations of the magnetic field are therefore only due to the different kinds of
19
20 136 errors which can then be minimized using a least squares method. The advantage of the
21
22 137 process is that it also compensates the remnant and induced magnetization of the device
23
24 138 itself (Munsch *et al.*, 2007). This makes the fluxgate the only magnetometer capable of
25
26 139 such compensation, allowing compact multi-sensor devices as well as motorized
27
28 140 measurements. A typical result of the effect of the calibration and compensation process
29
30 141 on a magnetometer is shown in Figure 4, where computed parameters reduce the
31
32 142 variations of measurements at a fixed point from around 200 nT to 0.3 nT.

33 34 35 36 37 38 39 40 41 42 43 44 45 46 47 48 49 50 51 52 53 54 55 56 57 58 59 60

143 *Time-dependant variations*

144 Another issue with the measurement of the total magnetic field is the correction of
145 the time-dependant variations which may be caused by extra-terrestrial sources or
146 anthropic activities. Additionally, fluxgate magnetometers are not absolute and subject
147 to drift with the change of temperature (0.1 to 0.5 nT/°C according to the manufacturer).
148 In an environment affected by homogeneous but not linear temporal variations, as it is
149 often the case in urban areas, corrections can be made by using a magnetometer
150 installed at a fixed point (base station) during the measurements, thus recording only the
151 time dependant part of the signal. Such solution was not possible in Qasr 'Allam due to
152 legal and logistical difficulties to have a base station on the site at the time of the study.
153 However, during the surveying hours (6 to 10 a.m.), time-dependant variations are
154 linear and can therefore be easily corrected. They are the result of a combination of
155 effects from a temperature drift as well as from far external sources of which the linear
156 variation is confirmed by using geomagnetic records of one of the nearest
157 INTERMAGNET observatory (Tamanrasset).

158 *Data processing*

1
2
3
4 159 The measurement provides the 3 calibrated components of the total magnetic field,
5
6 160 from which the total magnetic intensity is calculated. In archaeology the prime interest
7
8 161 is to measure/illustrate subtle spatial variations of the magnetic field. This is achieved
9
10 162 by observing the anomalies of the total magnetic field's intensity. The anomaly is
11
12 163 defined as the difference between the intensity of the measured magnetic field and the
13
14 164 regional field (Blakely, 1995, pp. 178-180). The latest is computed using the
15
16 165 International Geomagnetic Reference Field (IGRF) (Finlay *et al.*, 2010). The anomaly
17
18 166 of the intensity of the total magnetic field can then be displayed either as profiles or as
19
20 167 maps after a gridding computerized operation (D'Errico, 2005). The node distance of
21
22 168 the grid is usually set as half of the distance between each magnetometer, i.e. 0.25 m in
23
24 169 this study. After this procedure, the residual errors can lead to the appearance of a
25
26 170 levelling effect between profiles (Fedi and Florio, 2003). To solve this problem, the
27
28 171 differences at the crossing points between the values on magnetic profiles (in-lines) and
29
30 172 traverses (tie-lines) are measured. Then, a constant to apply to each profile is calculated
31
32 173 by a linear inversion to minimize the differences at the crossing points.

30 174 **Results**

31
32 175 The data acquisition over the Qasr 'Allam site took place in April and May 2012.
33
34 176 Through 200 km of survey lines, more than 800 km of georeferenced magnetic profiles
35
36 177 were recorded over an area about 340,000 m² (Figure 5).

37 178 *Maps of magnetic anomalies*

38
39 179 Usually, magnetic anomalies are represented using maps with a linear colour scale.
40
41 180 Those consist in attributing a colour or grey tone to each node of the grid according to
42
43 181 its value using a linear scale, as shown in Figure 6. Unfortunately, such a representation
44
45 182 is often not sufficient to show accurately all the anomalies of a site, as they can range
46
47 183 from a few to hundreds of nano-Tesla. A common solution to this problem is to display
48
49 184 multiple maps with different scales to understand the anomalies from the largest to the
50
51 185 smallest. Such a process might be time consuming and is not the most practical, as
52
53 186 several maps have to be observed at the same time. To overcome this problem, we
54
55 187 introduce another approach, the equi-populated mapping. An equi-populated map
56
57 188 consists in attributing a shade (or colour) to each node using a non-linear scale in such a

1
2
3
4 189 way that all the shades are evenly distributed on the map. Thus, both small and strong
5 190 magnetic anomalies can be represented on a unique map, as shown in Figure 7.

6
7 191 From both representations (Figure 6-7), different kind of anomalies can be observed
8
9 192 on the site. Depending on their wavelength and shape, they can be ranked as follows.

10
11 193 - **Dipolar anomalies:** the strongest one in the west is due to a metallic pole; the
12
13 194 others are due to pieces of metal which are scattered everywhere on the site,
14
15 195 showing no particular distribution.

16
17 196 - **Short wavelength lineation** (about 1 m and less): they are the most common
18
19 197 anomalies and can be sorted in different subgroups. In the southern part, a high
20
21 198 concentration of curved lines following roughly N-S and E-W orientations is
22
23 199 present. A similar pattern can be seen in the northern part, though in much
24
25 200 smaller quantities. In the central part, the lines are straighter and follow an
26
27 201 orientation similar to the one of the large wavelength lineation surrounding
28
29 202 them.

30
31 203 - **Large wavelength lineation** (about 10 m): they approximately draw two
32
33 204 rectangles of 150 x 100 and 125 x 100 m in the central part of the map. Their
34
35 205 orientation is of a few degrees east.

36
37 206 - **North-south gradient:** the magnetic anomaly field decreases of about 20 nT
38
39 207 from north to south. This gradient cannot be explained by the regional magnetic
40
41 208 field as the International Geomagnetic Reference Field gives an increase of 3.8
42
43 209 nT from north to south. Thus, it is likely that such a gradient is due to a deep
44
45 210 local variation of the underlying geology.

46
47 211 These anomalies reveal the presence of different kind of magnetic heterogeneities
48
49 212 within the ground. Unfortunately, the shape, amplitude and position of an anomaly (as
50
51 213 well as the gradient) depend on multiple factor such as the shape, the orientation, the
52
53 214 position and magnetization of the source as well as the orientation of the regional
54
55 215 magnetic field. To decipher these anomalies, interpretation tools can be found in
56
57 216 potential field theory.

58
59 217 *Potential field transformations*

60 218 In any kind of magnetometry, the horizontal position of the sources is situated
219 somewhere in between the positive and negative extrema of a skewed anomaly. When

220 the wavelength is shorter than the size of the object, as it is often the case for very
 221 shallow objects, this is not a problem. Otherwise, as it is often the case in this study, the
 222 error can reach up to a few metres, which is not acceptable to locate properly
 223 archaeological trenches. Fortunately, the position of the remains can be obtained by
 224 using a potential field transformation known as the double reduction to the pole (DRP).
 225 The DRP consists in the calculation of the signal when both the magnetization and
 226 regional field are set vertical. Thus the anomalies become symmetrical with their
 227 maxima above their sources (Baranov, 1957). In the spectral domain, the operation is
 228 easily done by multiplying the spectrum of the anomaly by

$$\left[\frac{i\sqrt{u^2 + v^2}}{au + bv + ic\sqrt{u^2 + v^2}} \right] \left[\frac{i\sqrt{u^2 + v^2}}{a'u + b'v + ic'\sqrt{u^2 + v^2}} \right], \quad (1)$$

229 where u and v are the wavelengths associated with x and y directions, $i^2 = -1$,
 230 (a, b, c) the components of the unit vector in the direction of the regional magnetic
 231 field, and (a', b', c') the components of the unit vector in the direction of the
 232 magnetization (Bhattacharyya, 1965). The direction of the regional field is given by the
 233 IGRF while the direction of magnetization is either set as the same as the regional field
 234 when the ratio remnant/induced magnetization is near zero or obtained through
 235 successive iterations until the signal become symmetrical. In Qasr 'Allam, as the
 236 buildings are made in mudbricks, the orientation of magnetization was set equal to that
 237 of the regional field. In Figure 8, the anomalies become symmetrical, confirming this
 238 induced-only magnetization hypothesis. It must be noted that a simple reduction to the
 239 pole (only one vector set vertical) does not give the position of the source (Figure 8).
 240 The calculated DRP map gives therefore the position of sources visible or not on the
 241 surface (Figure 9). The archaeological interpretation stays difficult due to the presence
 242 of a very large wavelength anomaly most probably due to the geology. An easy way to
 243 enhance the shortest wavelength while smoothing the largest ones is the use of the
 244 vertical derivative. The operation is straightforward in the spectral domain and
 245 corresponds to the multiplication of the spectrum of the map by

$$\left(\sqrt{u^2 + v^2} \right)^n, \quad (2)$$

1
2
3
4 246 where u and v are the wavelengths associated with x and y directions and n is the order
5
6 247 of derivation. Figure 10 corresponds to the map obtained after computing the vertical
7
8 248 gradient of the DRP. It can be observed that the different lines are indeed enhanced and,
9
10 249 most importantly, new lineations appear, especially in the central area.

11 *Comparison with gradiometry*

12
13 251 To assess the quality of the data for archaeological interpretation compared to
14
15 252 gradiometry, the area surveyed by Herbich (2011) with a fluxgate gradiometer (Geoscan
16
17 253 FM256) was also covered with the device developed in this study. The comparison of
18
19 254 the results (Figure 11) shows that the proposed method reveals at least as many
20
21 255 information as a vector gradiometer, even though the magnetometers are more distant
22
23 256 from the ground (1 m). The vertical derivative map (Figure 11, A) appears more blurred
24
25 257 than the gradiometric map (Figure 11, B) because it corresponds to a more distant
26
27 258 acquisition from the sources.

28 **Discussion**

29 *Interpretation of magnetic anomalies*

30
31 261 The different maps give important information on the sources of the magnetic
32
33 262 anomalies. The different linear anomalies can be interpreted as highly probable
34
35 263 archaeological remains and are divided into three categories: long wavelengths, straight
36
37 264 and non-straight short wavelengths. The non-straight linear elements with short
38
39 265 wavelengths follow the same rough orientation pattern and shape as the irrigation
40
41 266 structures visible on the ground surface. Some of them directly follow the traces of the
42
43 267 irrigation structures observed on the ground surface. They are also mostly connected to
44
45 268 an area of visible wells in the south eastern part of the site (Figures 2 and 5). This
46
47 269 strongly suggests that those anomalies can be interpreted as irrigation structures, present
48
49 270 not only under the sand dune, but also within the harder ground in the whole area
50
51 271 (Figure 12). A targeted excavation of such a structure within the sand dune (Figure 12,
52
53 272 area 15) confirmed open irrigation channels under 1.2 m of sediments (Colin and
54
55 273 Duvette 2012, pp. 163-164). The filling sediments of one segment contained artefacts
56
57 274 (potteries, terracotta figurines) of a well-attested type, according to the local typology of
58
59 275 the 8th or the 7th century B.C. (Colin and Duvette, 2012, p. 164). This information
60
276 validates the hypothesis that at least one part of the irrigation network was

1
2
3
4 277 contemporary to the cultic complex and that these farming devices most probably
5
6 278 belonged to the religious estate.

7 279 The two other types of linear anomalies can be interpreted differently. They are
8
9 280 situated in front of the access ramp of the platform, where the rest of a religious facility
10
11 281 can be expected. They show angular shapes, and display an orientation similar to the
12
13 282 one of the already excavated constructions. It can therefore be stated that they most
14
15 283 likely correspond to ancient buildings, thus enlarging the surface of the whole facility
16
17 284 from 40 000 m² to 150 000 m² (Figure 12). The variability of wavelengths can be
18
19 285 explained as different depths of sources, either due to the variability of the post-
20
21 286 abandonment sedimentary deposits, to different sizes of structures or to successive
22
23 287 archaeological periods. This is verified by two targeted excavations which started in
24
25 288 2013 and 2014 and are still in progress (Figure 12, areas 16 and 17). They revealed the
26
27 289 presence of cultic buildings corresponding to the magnetic anomalies at different depths
28
29 290 from 0.15 to 2.4 metres (Figure 12, area 16 and 17 respectively) which are related to
30
31 291 different occupations from at least the 8th or the 7th century B.C. to the 2nd century A.D.
32
33 292 and are affected by an environmental change (Colin, 2013b; Colin *et al.*, 2014). The
34
35 293 stratigraphy of the tested areas revealed that the sedimentary processes followed two
36
37 294 successive patterns. The ruins of the last occupation period (Roman times) are mainly
38
39 295 covered by aeolian sand in an arid context, but the remains of the former periods (from
40
41 296 Third Intermediate Period until Late Period or later) are filled with alluvial earthen
42
43 297 sediments, in a seemingly more humid context.

44 298 *The 3-axis fluxgate magnetometer total field approach*

45 299 In addition to the interpretation results, the study reveals the potential of the use of 3-
46
47 300 axis fluxgate magnetometers for large scale archaeological surveys. The light weight of
48
49 301 the magnetometers and their compensation ability allow the construction of a compact
50
51 302 multi-sensors device which can be operated by a single technician. At least four
52
53 303 simultaneous georeferenced magnetic data without any preliminary preparation of the
54
55 304 site can be acquired. The position of the magnetometers 1 m above the ground surface
56
57 305 allow to cover areas with more vegetation or a more uneven topography than with a
58
59 306 gradiometer device. Using vertical gradiometry, the lower probe is usually situated 0.2-
60
307 0.3 m above the ground surface. Thus, the proposed approach proved to be capable to
308
survey 5000 to 12000 m² per hour with a 0.5 m spacing and reveal at least as many

1
2
3
4 309 information on archaeological remains as a gradiometer through the use of the vertical
5 310 derivative of the signal (Figure 11). The application of the DRP gives theoretically the
6 311 exact horizontal position of the sources, unlike a single reduction which leads to a
7 312 residual skewness. If the difference or even the use of a reduction can be negligible for
8 313 very shallow sources, it is not the case with deeper sources, as shown in Figure 8 and
9 314 the comparison between Figure 7 and 9.

315 **Conclusion**

316 The study both validates the application of an innovative approach to magnetic
317 prospections in archaeology and reveals important information on the site of Qasr
318 'Allam.

319 The use 3-axis fluxgate magnetometers and associated potential field
320 transformations proved to be efficient to reveal information on both deep and shallow
321 archaeological sources at a large and rapid scale. The results obtained in Qasr 'Allam
322 offer two prospects for further development: 1- doubling the speed of acquisition by
323 doubling the number of magnetometers; 2- using the compensation ability to develop a
324 smaller device which allows a few centimetres spacing between sensors for high
325 precision small scale surveys.

326 In Qasr 'Allam, the geophysical survey strengthens the hypothesis of the
327 archaeologists. It locates remains of large scale buildings positioned in the expected
328 area, whose general plan and direction are consistent with the hypothesis of a religious
329 complex which combines a main cultic centre (totally covered by sediments) with
330 economic and domestic facilities (of which parts were previously excavated). The
331 accurate positioning of probable archaeological structures has allowed setting up
332 targeted excavations that led to important results: parts of the irrigation network were
333 already used from the 8th or 7th century B.C. in the vicinity of the buildings, the site was
334 used for cultic purposes to at least the 2nd century B.C. and was impacted by a rapid
335 environmental change from humid to arid in the latest periods of occupation. Without
336 the results provided by the magnetic mapping, the thickness of the sedimentary deposits
337 would have discouraged any attempt to explore the underground by means of the
338 classical archaeological digging methods. A next step would be to investigate further
339 the supposed cultic centre and the associated environmental change to find further
340 chronological and functional data. According to its size and the thickness of sediment,

1
2
3
4 341 the study would need the combination of archaeological excavations and a more
5
6 342 detailed geophysical method. In consequence, these conclusions encouraged the
7
8 343 Egyptian Supreme Council of Antiquities (SCA) to delimit an area to be protected in
9
10 344 2014 to avoid the destruction of remains by the fast progression of agricultural fields.

11 **Acknowledgement**

12
13 345 Some of the results presented in this paper rely on the data collected at Tamanrasset
14
15 346 observatory. We thank Centre de Recherche en Astronomie, Astrophysique et
16
17 347 Geophysique as well as Institut de Pysique du Globe de Paris, for supporting its
18
19 348 operation and INTERMAGNET for promoting high standards of magnetic observatory
20
21 349 practice (www.intermagnet.org). The authors would like to thank the Initiatives
22
23 350 d'Excellence (IdEx, Programme Investissements d'Avenir) of the University of
24
25 351 Strasbourg for their financial support as well as Laurent Ameglio, Daniel Sauter,
26
27 352 Nicolas Florsch, Chris Gaffney and the two anonymous reviewers for their advices and
28
29 353 constructive comments.
30
31 354

32 **References**

- 33 355 Baranov V. 1957. A new method for interpretation of aeromagnetic maps: pseudo-
34
35 356 gravimetric anomalies. *Geophysics* **22**: 359–383. DOI: 10.1190/1.1438369
36
37 357
38 358 Bhattacharyya BK. 1965. Two-dimensional harmonic analysis as a tool for magnetic
39
40 359 interpretation. *Geophysics* **30**: 829–857. DOI: 10.1190/1.1439658
41
42 360 Blakely RJ. 1995. *Potential Theory in Gravity and Magnetic Applications*. Cambridge
43
44 361 University Press. ISBN: 0-521-41508-X
45
46 362 Colin F. 2006. Bahariya. In: Pantalacci L, Denoix S (Eds.), Travaux de l'Institut
47
48 363 Français d'Archéologie Orientale en 2005-2006. *Bulletin de l'Institut Français*
49
50 364 *d'Archéologie Orientale* **106**: 404-409.
51
52 365 Colin F. 2010. Bahariya. In: Midant-Reynes B, Denoix S (Eds.), Travaux de l'Institut
53
54 366 Français d'Archéologie Orientale en 2009-2010. *Bulletin de l'Institut Français*
55
56 367 *d'Archéologie Orientale* **110**: 326-331.
57
58 368 Colin F. 2011. Le «Domaine d'Amon» à Bahariya de la XVIII^e à la XXVI^e dynastie :
59
60 369 l'apport des fouilles de Qasr 'Allam. in: Devauchelle D. (Ed.), *La XXVI^e Dynastie*
370 *Continuités et Ruptures. Actes Du Colloque International Organisé Les 26 et 27*
371 *Novembre 2004 à l'Université Charles-de-Gaulle – Lille 3. Promenade Saïte Avec Jean*
372 *Yoyotte*: 47 – 84. Paris.

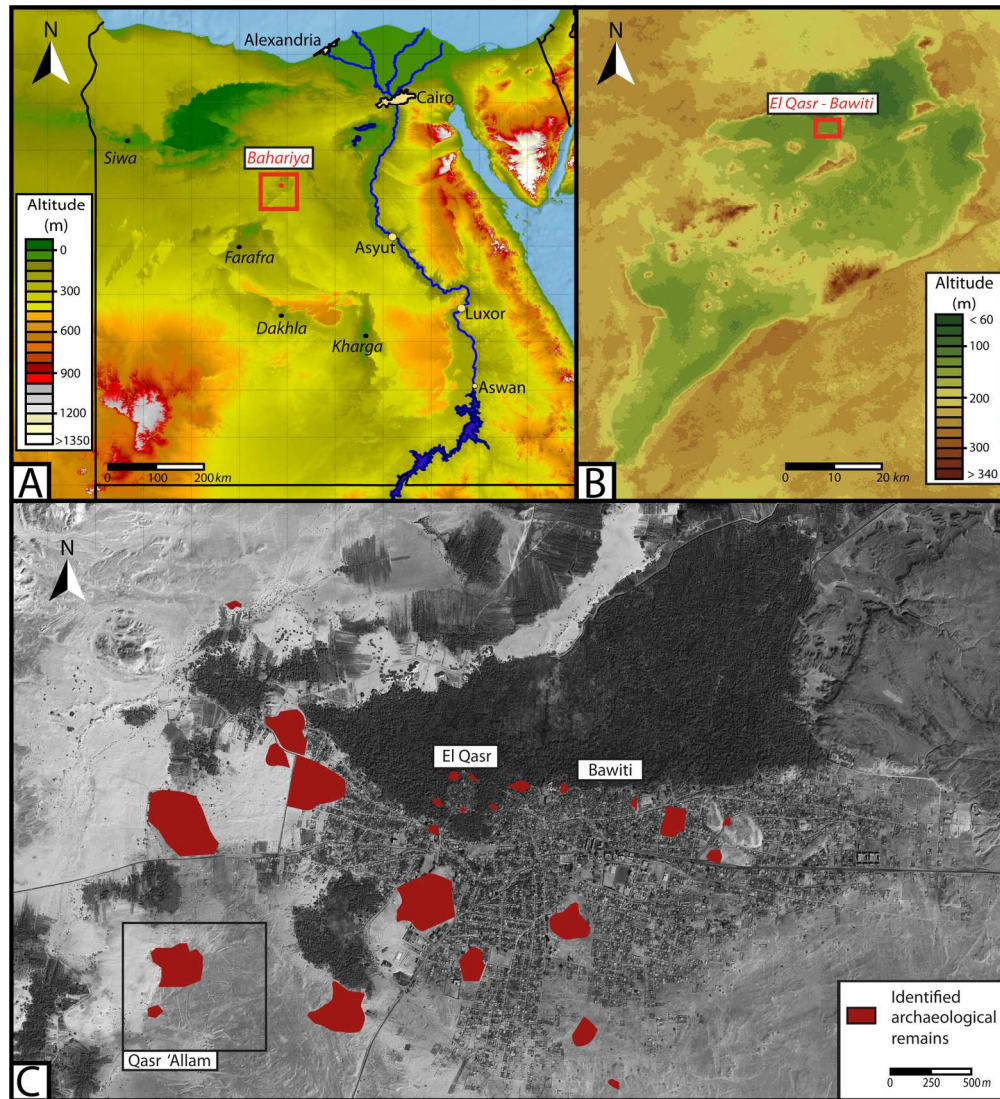
- 1
2
3
4 373 Colin F. 2013a. Les gisements archéologiques de Psôbthis au début du XXI^e siècle :
5 374 Diagnostic sur un paysage menacé et nouvelles orientations de recherche. in: Dospěl,
6 375 M., Suková, L (Eds.). *Bahriya Oasis: Recent Research into the Past of an Egyptian*
7 376 *Oasis*: 151–184. Charles University; Prague.
- 9 377 Colin F. 2013b. Bahariya. Pratiques funéraires et lieux de culte. In: Midant-Reynes B
10 378 (Ed.). Rapport d'activité 2012-2013, *Supplément au Bulletin de l'Institut Français*
11 379 *d'Archéologie Orientale* **113**: 246–251.
- 13 380 Colin F, Duvette C. 2012. Bahariya. Pratiques funéraires et lieux de culte. In: Midant-
14 381 Reynes B (Ed.). Rapport d'activité 2011-2012, *Supplément au Bulletin de l'Institut*
15 382 *Français d'Archéologie Orientale* **112**: 159–165.
- 17 383 Colin F, Duvette C, Gavazzi B, Munsch M, Schuster M, Schwarz D. 2014. Bahariya.
18 384 Pratiques funéraires et lieux de culte. In: Midant-Reynes B (Ed.). Rapport d'activité
19 385 2013-2014, *Supplément au Bulletin de l'Institut Français d'Archéologie Orientale* **114**:
20 386 195–201.
- 22 387 Colin F, Labrique F. 2003. Recherches de terrain en Égypte. Chronique. *Dialogues*
23 388 *d'histoire ancienne* **29** (2): 165-185. DOI: 10.3406/dha.2003.1569
- 25 389 D'Errico J. 2005. Surface Fitting using gridfit.
26 390 (<http://www.mathworks.com/matlabcentral/fileexchange/loadFile.do?objectId=8998>),
27 391 MATLAB Central File Exchange.
- 29 392 Fagaly R L. 2001. Superconducting Quantum Interference Devices (SQUIDS). In: Ripka
30 393 P (Ed). *Magnetic Sensors and Magnetometers*: 305-347. Artech House. ISBN: 1-58053-
31 394 057-5
- 33 395 Fedi M, Florio G. 2003. Decorrugation and removal of directional trends of magnetic
34 396 fields by the wavelet transform: application to archaeological areas. *Geophysical*
35 397 *Prospecting* **51**: 261–272. DOI: 10.1046/j.1365-2478.2003.00373.x
- 37 398 Finlay CC, Maus S, Bondar TN, Chambodut A, Chernova TA, Chulliat A, Golovkov
38 399 VP, Hamilton B, Hamoudi M, Holme R, Hulot G, Kuang W, Langlais B, Lesur V,
40 400 Lowes FJ, Lühr H, Macmillan S, Manda M, McLean S, Manoj C, Menvielle M,
41 401 Michaelis I, Olsen N, Rauberg J, Rother M, Sabaka TJ, Tangborn A, Tøffner-Clausen
42 402 L, Thébaud E, Thomson AWP, Wardinski I, Wei Z, Zvereva TI. 2010. International
43 403 Geomagnetic Reference Field: the eleventh generation. *Geophysical Journal*
44 404 *International* **183**: 1216–1230. DOI: 10.1111/j.1365-246X.2010.04804.x
- 46 405 Gaffney C. 2008. Detecting Trends in the Prediction of the Buried Past: A Review of
47 406 Geophysical Techniques in Archaeology. *Archaeometry* **50**: 313–336. DOI:
48 407 10.1111/j.1475-4754.2008.00388.x
- 50 408 Herbich T. 2011. Geophysical surveying in Egypt: periodic report for 2009-2011. in:
51 409 Drahor MG, Berge MA. *Archaeological Prospection. 9th International Conference on*
52 410 *Archaeological Prospection, September 19-24, 2011 Izmir (Turkey)*: 234-239. Istanbul.

- 1
2
3
4 411 Jarvis A, Reuter HI, Nelson A, Guevara E. 2008. Hole-filled seamless SRTM data V4.
5 412 *International Centre for Tropical Agriculture (CIAT)*. available from
6 413 <http://srtm.csi.cgiar.org>.
- 7
8 414 Leclère F. 2008. *Les villes de Basse Égypte au Ier millénaire av. J.-C. Analyse*
9 415 *archéologique et historique de la topographie urbaine*. Bibliothèque d'étude 144/2.
10 416 IFAO. Le Caire. ISBN: 978-2-7247-0491-4
- 11
12 417 Linford N. 2006. The application of geophysical methods to archaeological prospection.
13 418 *Reports on Progress in Physics* **69**: 2205–2257. DOI: 10.1088/0034-4885/69/7/R04
- 14
15 419 Malecka-Drozd N. 2014. The emergence and development of architecture on the
16 420 casemate foundation platforms in the Nile Delta. *Recherches Archéologiques Nouvelle*
17 421 *Série* **4**: 69-96.
- 18
19 422 Munsch M, Boulanger D, Ulrich P, Bouiflane M. 2007. Magnetic mapping for the
20 423 detection and characterization of UXO: Use of multi-sensor fluxgate 3-axis
21 424 magnetometers and methods of interpretation. *Journal of Applied Geophysics* **61**: 168–
22 425 183. DOI: 10.1016/j.jappgeo.2006.06.004
- 23
24 426 Nabighian MN, Grauch VJS, Hansen RO, LaFehr TR, Li Y, Peirce JW, Phillips JD,
25 427 Ruder ME. 2005. 75th Anniversary: The historical development of the magnetic method
26 428 in exploration. *Geophysics* **70**: 33–61. DOI: 10.1190/1.2133784
- 27
28 429 Olsen N, Tøffner-Clausen L, Sabaka TJ, Brauer P, Merayo JMG, Jørgensen JL, Léger
29 430 JM, Nielsen OV, Primdahl F, Risbo T. 2003. Calibration of the Ørsted vector
30 431 magnetometer. *Earth, Planets, and Space* **55**: 11–18. DOI: 10.1186/BF03352458
- 31
32 432 Primdahl F. 1979. The fluxgate magnetometer. *Journal of Physics E: Scientific*
33 433 *Instruments* **12**: 241-253. DOI: 10.1088/0022-3735/12/4/001
- 34
35 434 Spencer AJ. 1979a. *Brick architecture in Ancient Egypt*. Aris & Philips; Warminster.
36 435 ISBN: 0856681288
- 37
38 436 Spencer AJ. 1979b. The brick foundations of Late Period peripteral temples and their
39 437 mythological origin. In: Ruffle J, Gaballa G, Kitchen K (Eds). *Glimpses of Ancient*
40 438 *Egypt. Studies in Honour of H.W. Fairman*: 132-137. Aris & Philips; Warminster.
- 41
42 439 Svoboda JA. 2006. Prehistory of the southern Bahariya Oasis, Western Desert, Egypt.
43 440 An outline. *Archaeology, Ethnology and Anthropology of Eurasia* **28**: 18–30. DOI:
44 441 10.1134/s1563011006040037
- 45
46 442 Svoboda JA. 2013. Prehistory of the Southern Bahariya: A case Study in Northeast
47 443 African Settlement Archaeology. in Dospěl, M., Suková, L. (Eds.), *Bahriya Oasis.*
48 444 *Recent Research into the Past of an Egyptian Oasis*: 35-62. Charles University; Prague.
- 49
50 445 Traunecker M. 1987. Les "temples hauts" de Basse époque : un aspect du
51 446 fonctionnement économique des temples, *Revue d'égyptologie* **38**: 147–162. DOI:
52 447 10.2143/RE.38.0.2011639
- 53
54
55
56
57
58
59
60

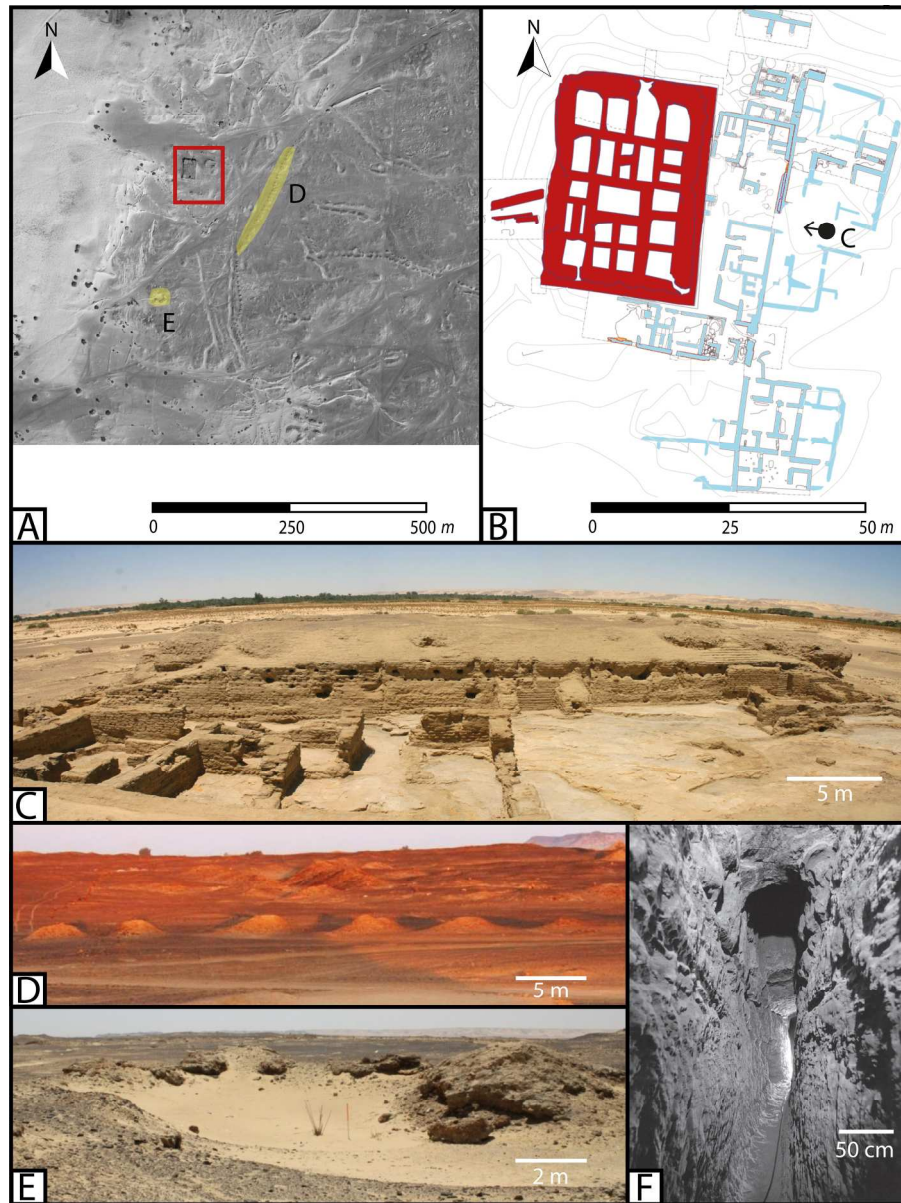
1
2
3
4 448 Wuttman M, Bousquet B, Chauveau M, Dils P, Marchand S, Schweitzer A, Volay L.
5 449 1996. Premier rapport préliminaire des travaux sur le site de 'Ayn Manawir (oasis de
6 450 Kharga). *Bulletin de l'Institut Français d'Archéologie Orientale* **96**: 385 – 451.

7
8 451
9
10
11
12
13
14
15
16
17
18
19
20
21
22
23
24
25
26
27
28
29
30
31
32
33
34
35
36
37
38
39
40
41
42
43
44
45
46
47
48
49
50
51
52
53
54
55
56
57
58
59
60

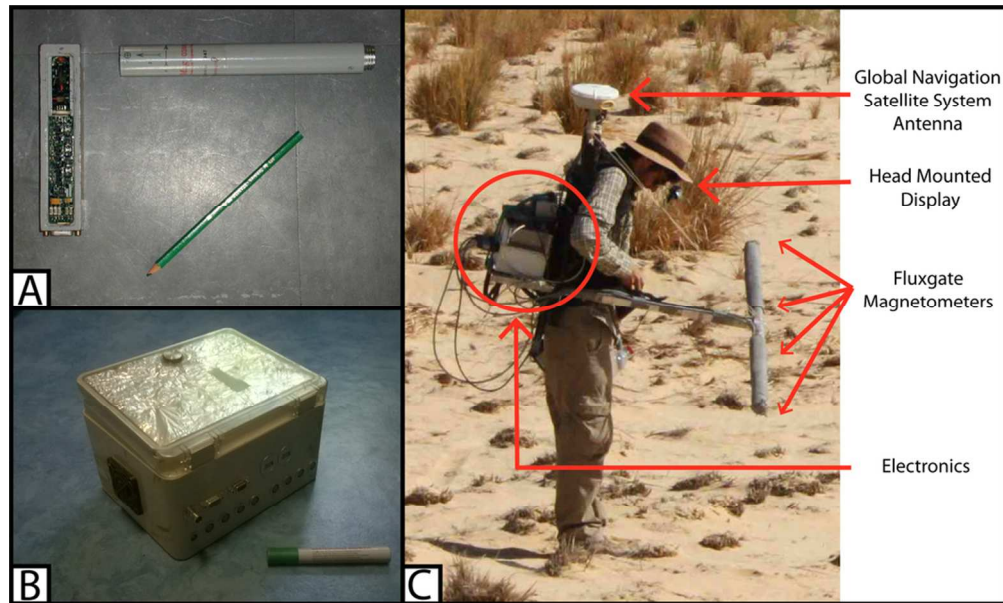
For Peer Review Only



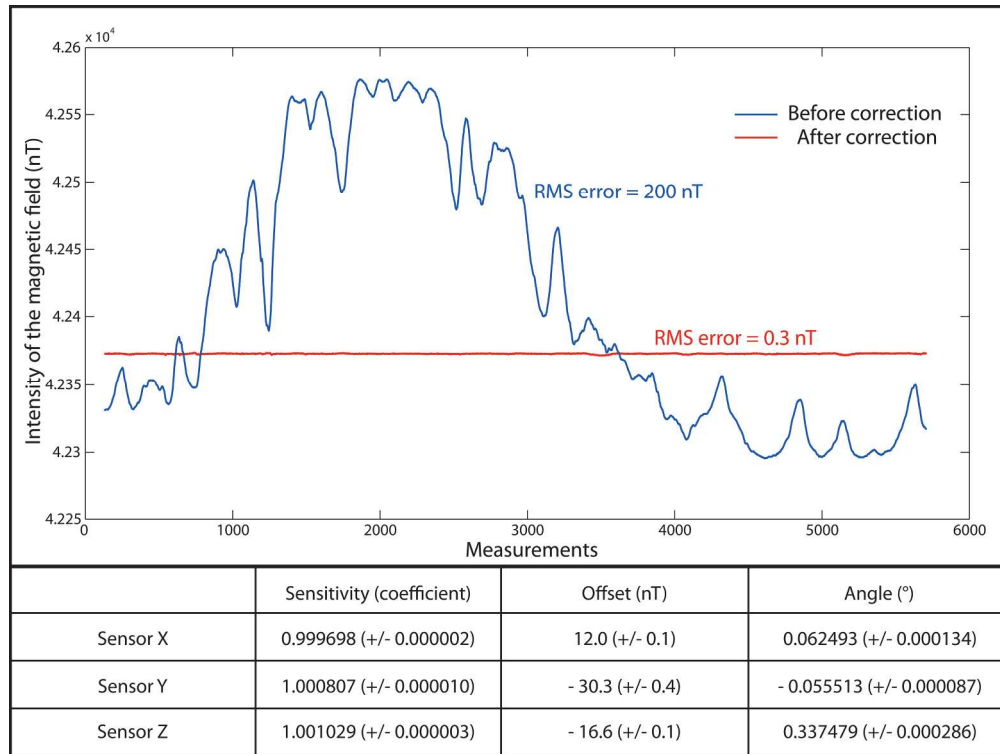
A- Localization of the oasis of Bahariya on a topographic map of Egypt. B- Localization of El Qasr-Bawiti on a topographic map of Bahariya. C- Localization of the site of Qasr 'Allam on a satellite image of El Qasr and Bawiti. Topography from SRTM90 data available at <http://srtm.csi.cgiar.org/> (Jarvis et al., 2008). Satellite image from the satellites Quickbird taken in 2003 (DigitalGlobe Incorporated, Eurimage SPA licence).
164x180mm (300 x 300 DPI)



A- Localization of the excavated dwelling (red) and the irrigation structures of the pictures D and E (yellow) on a satellite image of Qasr 'Allam (DigitalGlobe Incorporated, Eurimage SPA licence). B- Architectural plan of the excavated dwelling and orientation of the picture C. Blue and red colours corresponds to buildings of a first and second period of occupation. C- Lateral view of the cellular foundation platform of the second period of occupation. D- Traces of an underground channel. E- Traces of a well. F- Inside of an underground channel similar to the ones of the site and excavated in the oasis of Kharga (Wuttman et al., 1996).
199x265mm (300 x 300 DPI)

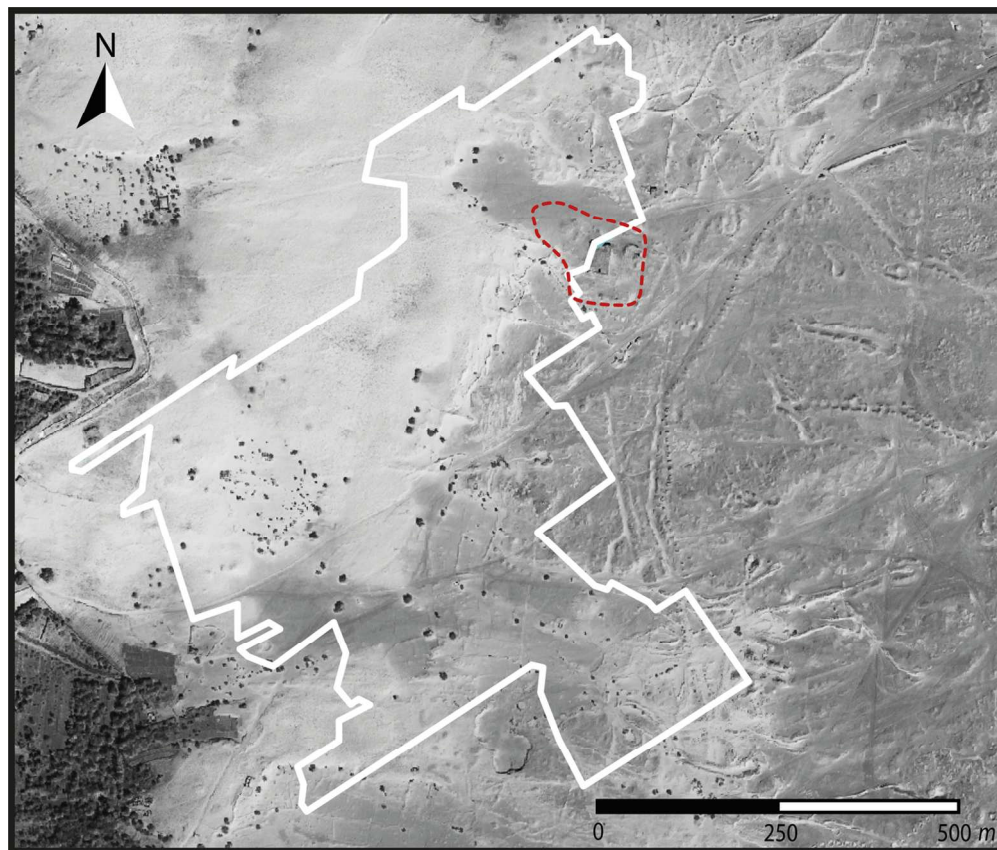


A- 3-axis fluxgate magnetometer (Bartington Inc., Mag-03 MC). B- Custom electronics with 8 magnetometer inputs developed by Institut de Physique du Globe de Strasbourg (IPGS). C- Multi-sensor device developed by IPGS.
90x54mm (300 x 300 DPI)



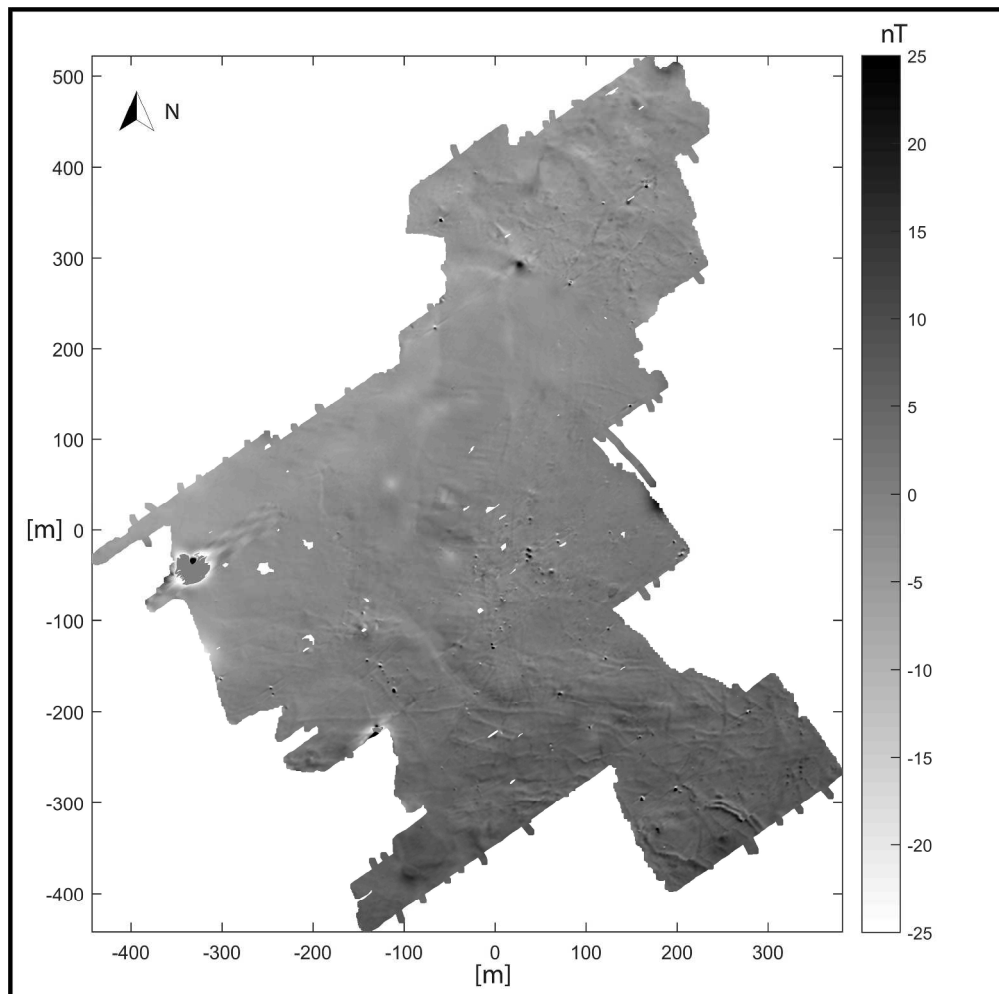
Intensity of the magnetic field measured by one magnetometer during the calibration and compensation process of the device before (blue) and after (red) corrections. Computed error parameters are given in the lower part of the figure.
112x85mm (600 x 600 DPI)

Manuscript Only



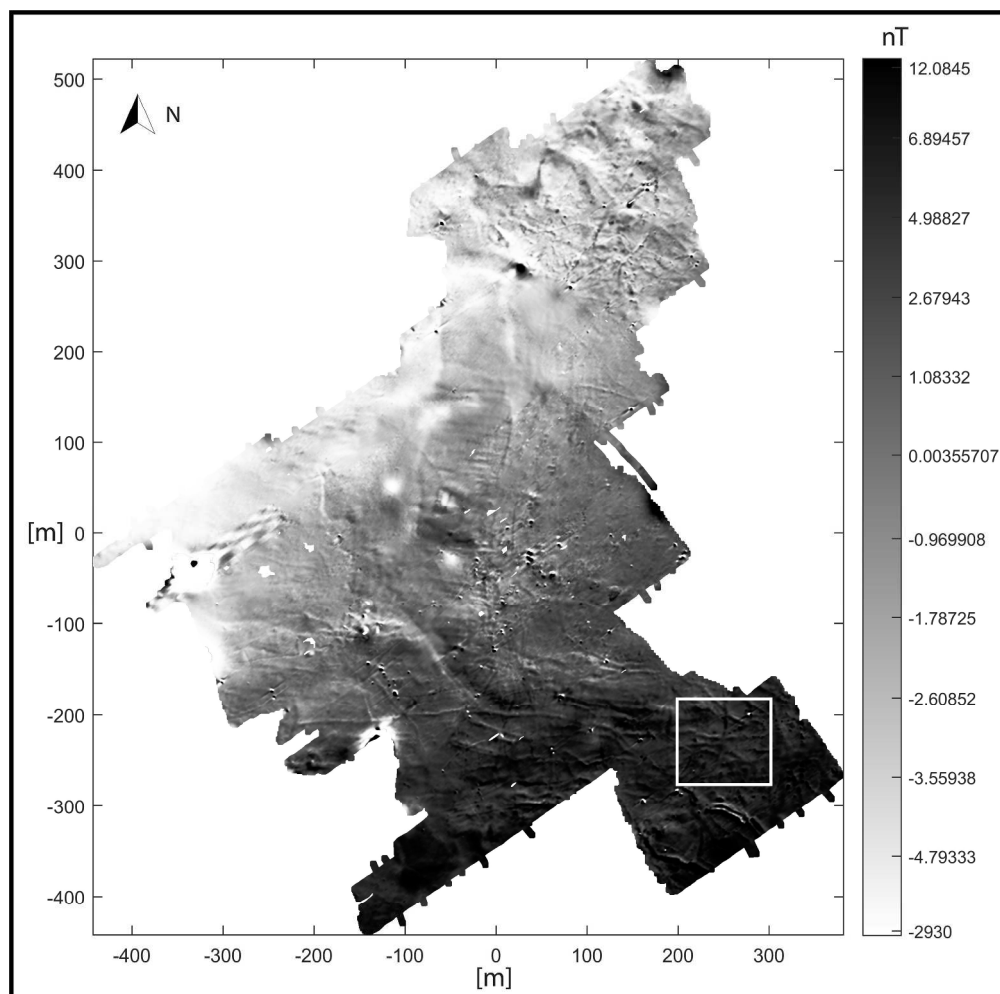
Satellite image of Qasr 'Allam (DigitalGlobe Incorporated, Eurimage SPA licence). The area of the geomagnetic prospection is delimited by the white line. The area of the excavated dwelling is delimited by the red line.
126x107mm (300 x 300 DPI)

1
2
3
4
5
6
7
8
9
10
11
12
13
14
15
16
17
18
19
20
21
22
23
24
25
26
27
28
29
30
31
32
33
34
35
36
37
38
39
40
41
42
43
44
45
46
47
48
49
50
51
52
53
54
55
56
57
58
59
60

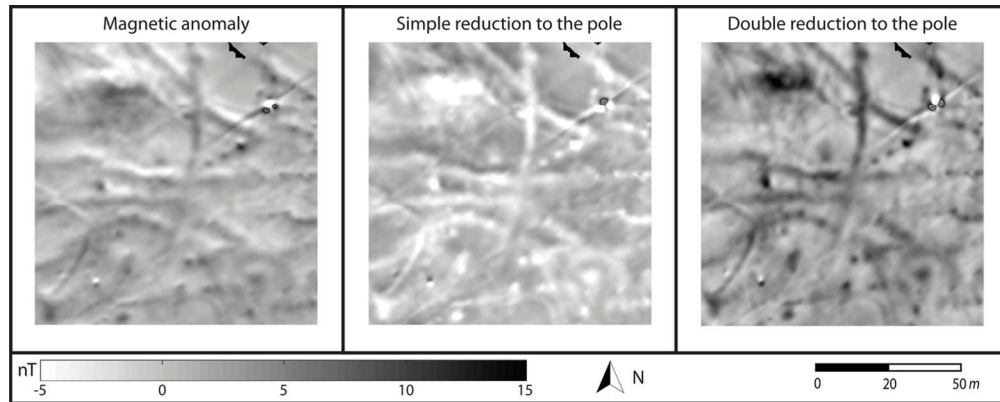


Map of the magnetic anomaly represented with a linear grayscale bar ranging from -25 to 25 nT.
148x147mm (600 x 600 DPI)

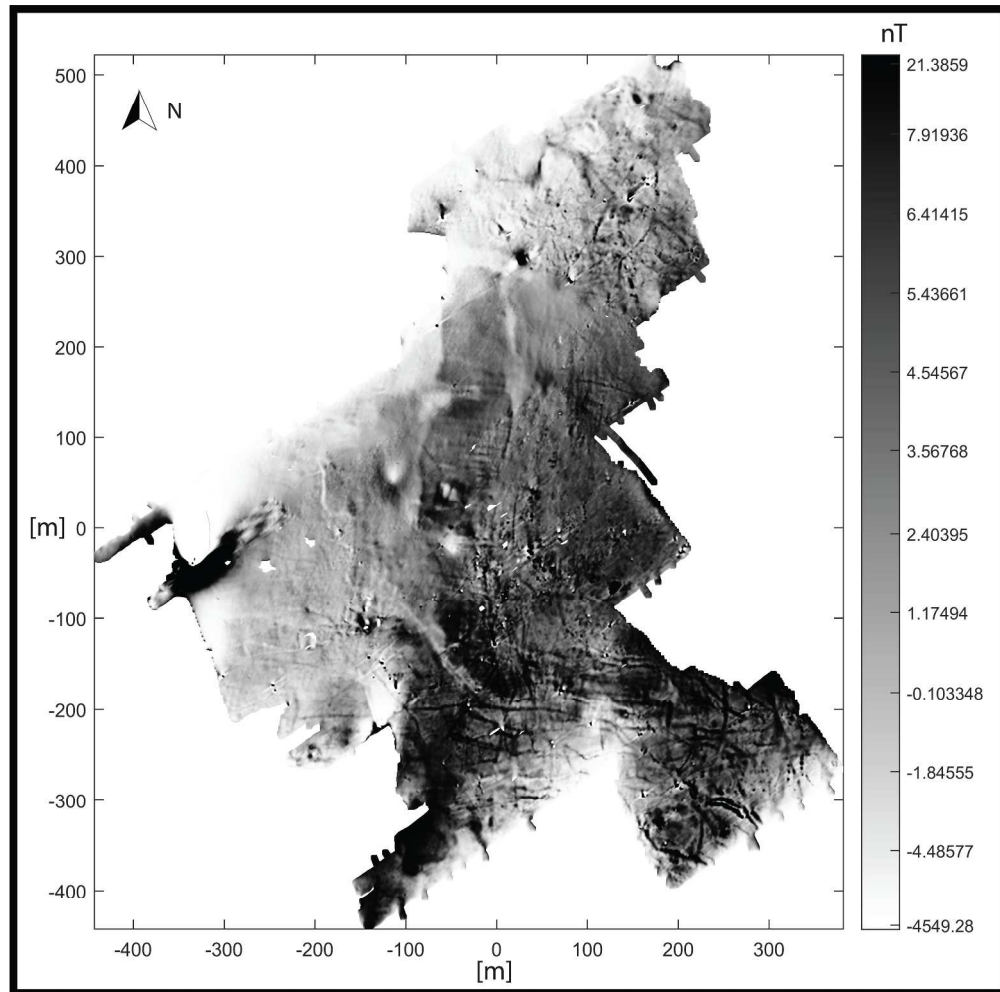
only



Map of magnetic anomalies represented with an equi-populated greyscale bar. The area delimited by the white line corresponds to the area displayed in Figure 8.
148x147mm (600 x 600 DPI)

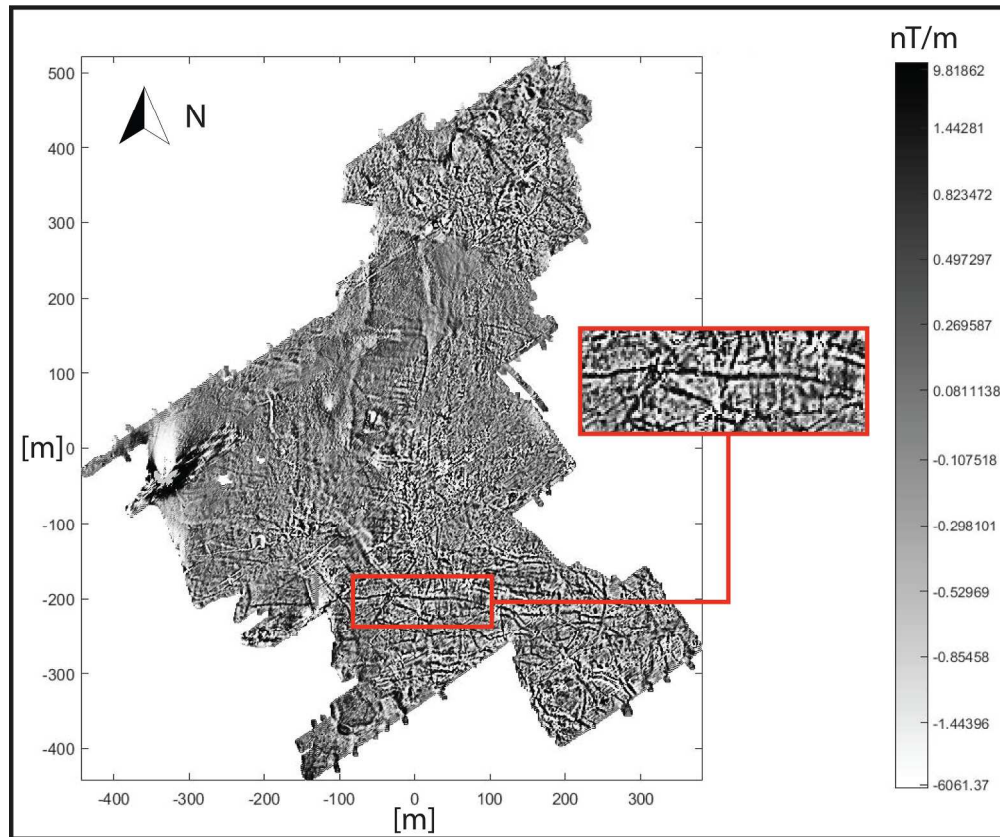


From left to right, map of the magnetic anomaly for a sampled zone of Qasr 'Allam (Figure 7), reduction to the pole of the regional magnetic field and double reduction to the pole. The IGRF-11 was used to obtain the direction to the regional magnetic field and the magnetization direction is set equal to the IGRF direction.
59x23mm (600 x 600 DPI)

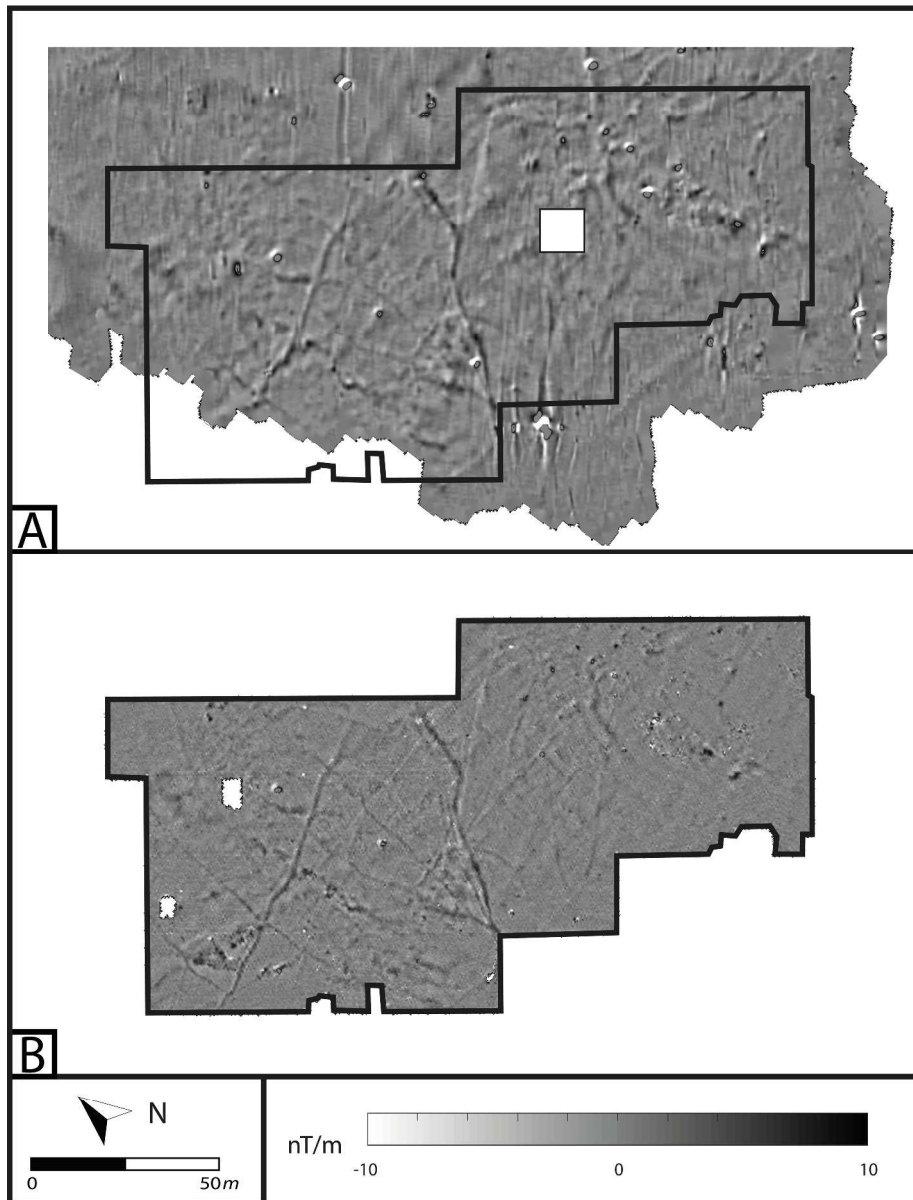


Map of the magnetic anomaly after double reduction to the pole represented with an equi-populated greyscale bar.
148x147mm (600 x 600 DPI)

1
2
3
4
5
6
7
8
9
10
11
12
13
14
15
16
17
18
19
20
21
22
23
24
25
26
27
28
29
30
31
32
33
34
35
36
37
38
39
40
41
42
43
44
45
46
47
48
49
50
51
52
53
54
55
56
57
58
59
60

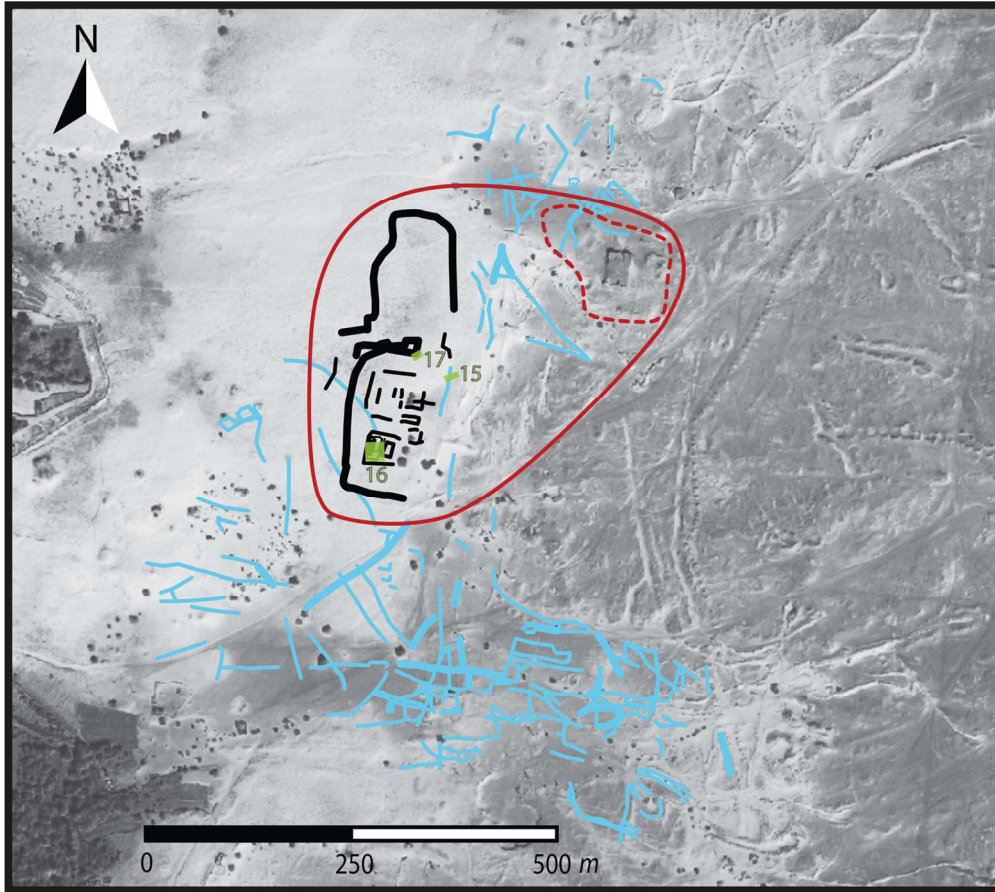


Map of the vertical derivative of the magnetic anomaly after double reduction to the pole represented with an equi-populated greyscale bar. The enlargement corresponds to the area delimited in red. 125x104mm (600 x 600 DPI)



A- Map of the vertical gradient computed from the data measured with the device developed by Institut de Physique de Globe de Strasbourg (using a vertical derivative). B- Map of the vertical gradient computed from the data measured by teams directed by Tomasz Herbich with a vector gradiometer Geoscan FM256 during previous surveys (Herbich 2011).
196x257mm (600 x 600 DPI)

1
2
3
4
5
6
7
8
9
10
11
12
13
14
15
16
17
18
19
20
21
22
23
24
25
26
27
28
29
30
31
32
33
34
35
36
37
38
39
40
41
42
43
44
45
46
47
48
49
50
51
52
53
54
55
56
57
58
59
60



Interpretative map of the archaeological remains from the geomagnetic prospection. The hydraulic structures are represented in blue, the buildings in black. The dotted and plain red lines mark the minimal limits of the dwelling known before and after the study. The areas highlighted in green correspond to three excavations numbered 15, 16 and 17.

133x119mm (300 x 300 DPI)

Only